



# CHORUS

This is the accepted manuscript made available via CHORUS. The article has been published as:

## Positronium collisions with molecular nitrogen

R. S. Wilde and I. I. Fabrikant

Phys. Rev. A **97**, 052708 — Published 15 May 2018

DOI: [10.1103/PhysRevA.97.052708](https://doi.org/10.1103/PhysRevA.97.052708)

# Positronium collisions with molecular nitrogen

R. S. Wilde<sup>1</sup> and I. I. Fabrikant<sup>2</sup>

<sup>1</sup>*Department of Natural Sciences, Oregon Institute of Technology,*

*Klamath Falls, Oregon 97601, USA*

<sup>2</sup>*Department of Physics and Astronomy,*

*University of Nebraska, Lincoln, Nebraska 68588-0299, USA*

## Abstract

For many atomic and molecular targets positronium (Ps) scattering looks very similar to electron scattering if total scattering cross sections are plotted as functions of the projectile velocity. Recently this similarity was observed for the resonant scattering by the N<sub>2</sub> molecule. For correct treatment of Ps-molecule scattering incorporation of the exchange interaction and short-range correlations is of paramount importance. In the present work we have used a free-electron-gas model to describe these interactions in collisions of Ps with the N<sub>2</sub> molecule. The results agree reasonably well with the experiment, but the position of the resonance is somewhat shifted towards lower energies, probably due to the fixed-nuclei approximation employed in the calculations. The partial-wave analysis of the resonant peak shows that its composition is more complex than in the case of  $e$ -N<sub>2</sub> scattering.

PACS numbers:

## I. INTRODUCTION

The observed similarity between electron and Ps scattering by neutral targets [1–3] was recently extended to resonant scattering in Ps-N<sub>2</sub> [3, 4] and Ps-CO<sub>2</sub> [2] collisions. In particular the very well-known resonance in  $e$ -N<sub>2</sub> scattering of the  $\Pi_g$  symmetry [5] looks very similar to the observed resonance in the Ps-N<sub>2</sub> scattering if cross sections for both processes are plotted as functions of the projectile velocity. This similarity prompts a theoretical question if the observed phenomenon is universal, that is can one predict with confidence that there is a resonance in Ps-molecule scattering if a resonance is observed in electron-molecule scattering?

The  $\Pi_g$  resonance in  $e$ -N<sub>2</sub> scattering has been studied in many theoretical and experimental papers, and it served in fact as a “workhorse” for many theoretical models of resonant electron-molecule collisions. (For a review of early work on the resonant  $e$ -N<sub>2</sub> collisions see [5]). Theoretical papers on  $e$ -N<sub>2</sub> resonant scattering can be separated into two categories: calculations performed in the fixed-nuclei approximations [6–11] and calculations which account for vibrational motion [12–17]. In the second class of calculations a single resonance is split into series of peaks, so-called boomerang oscillations [13], which appear because the resonance lifetime is comparable with the vibrational period in N<sub>2</sub>.

The importance of resonance phenomena in electron-molecule collisions cannot be overemphasized since resonances drive many inelastic processes in these collisions, particularly vibrational excitation and dissociative electron attachment [18, 19]. Therefore, if similar resonances exist in Ps-molecule collisions, they can drive similar processes, particularly Ps-impact vibrational excitation and dissociative Ps attachment.

A recent experimental paper [4] confirmed earlier predictions [3] of the resonant Ps-N<sub>2</sub> scattering and extended previous measurements towards the challenging region of low Ps energies. In interpreting their results, the authors [4] assumed that the electron, on the average, is closer to the target than the positron [20], and averaged the electron scattering cross section for N<sub>2</sub> over the momentum distribution of electron in Ps. The result of this convolution exhibits a resonance peak which is somewhat too broad as compared to the experimental data. As will be shown in the present paper, the idea of Ps-electron-target-electron correlation is justified by the proper treatment of the exchange interaction and short-range Ps-target correlations. However, the distortion of Ps by the target due to the long-

range electrostatic interaction should be treated simultaneously with the target distortion. This leads particularly to the van der Waals force at large distances.

To account for the Pauli exclusion principle, much effort was done in the past to enforce orthogonality between the wavefunction of the Ps electron and the target electrons by using orthogonalizing pseudopotentials [21–23] and orthogonal exchange kernels [24–26]. In our previous pseudopotential treatment of Ps collisions [27–30] we mocked the orthogonality constraint by using pseudopotentials with repulsive cores. However, for the complete inclusion of exchange in electron-molecule collisions the orthogonality constraint is not sufficient. The exchange interaction contains a substantial attractive component due to the so-called Fermi hole, and is particularly responsible for the  $\Pi_g$  resonance in electron-N<sub>2</sub> scattering [5, 10]. Inclusion of electron exchange in Ps collisions with atoms and molecules in a completely *ab initio* way is a very challenging task [31], and has been accomplished only for simple targets such as the hydrogen atom [32, 33] and rare-gas atoms [34–37]. An even more challenging problem is incorporation of short-range correlations in Ps-atom and Ps-molecule scattering. A recent work of Green *et al.* [37] incorporated them in Ps-rare-gas-atom scattering in the lowest order of perturbation theory. It seems reasonable that higher-order corrections are not significant in this case, and this justifies the perturbative approach used in the present paper.

In the present paper we use the free-electron-gas (FEG) exchange and correlation energies obtained in the previous paper of this series [38] to construct exchange and correlation potentials for Ps-N<sub>2</sub> scattering and calculate Ps-N<sub>2</sub> scattering cross sections in the fixed-nuclei approximation. This is a necessary first step in treatment of Ps-N<sub>2</sub> scattering before incorporation of the vibrational dynamics. The orthogonality constraint is not important for the resonant scattering since there is no occupied  $\pi_g$  orbital in the N<sub>2</sub> molecule, therefore we do not include it.

The rest of the paper is organized as follows. In Sec. II we present exchange and correlation potentials for Ps-N<sub>2</sub> scattering. In Sec. III we describe our calculations of Ps ionization in Ps-N<sub>2</sub> collisions. In Sec. IV we present the results for elastic and total scattering cross sections. We then turn to conclusions and an outlook. Atomic units are used throughout unless stated otherwise.

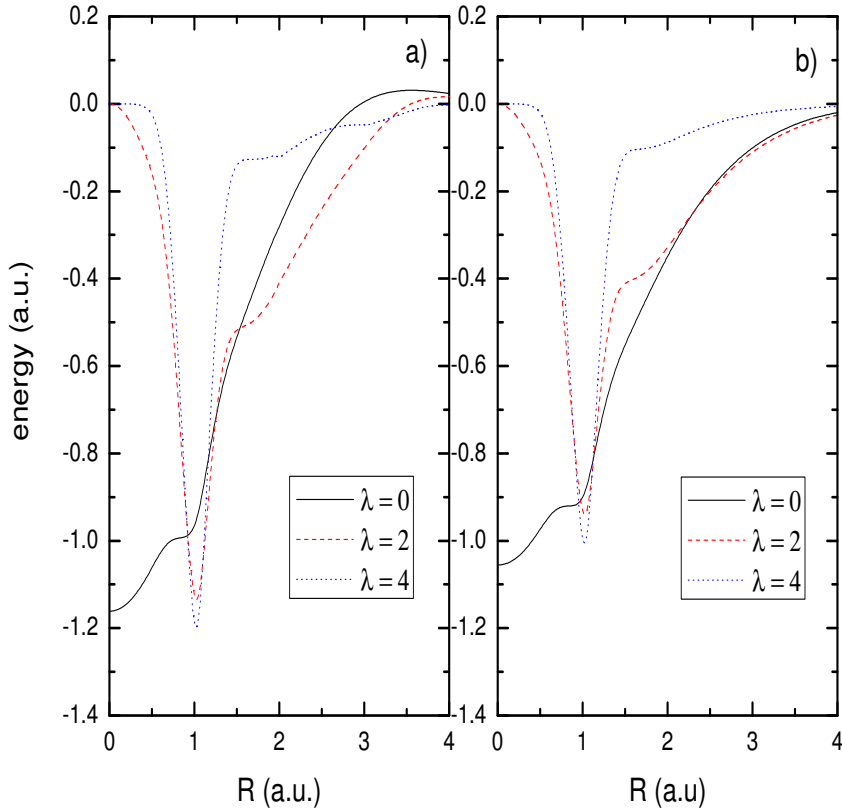


FIG. 1: (Color online) Legendre components of Ps-N<sub>2</sub> scattering potentials. a) Exchange potential. b) Correlation potential.

## II. SCATTERING POTENTIALS

In the previous paper [38] we have derived expressions for the exchange and correlation energies as functions of the Fermi energy. In order to introduce the dependence of these energies on the projectile position relative to the target we determine the Fermi energy in terms of the charge density of N<sub>2</sub> using the near Hartree-Fock wave-functions of Cade *et al.* [39]. The Ps-N<sub>2</sub> scattering potentials obtained in this way are then expanded in Legendre polynomials. In Fig. 1 we show the lowest three components ( $\lambda=0,2,4$ ) of this expansion for both the exchange and correlation potentials for a velocity of 0.05 a.u., the total potential is obtained by summing these.

The correlation potential at large distances is matched to the van der Waals potential with a cut-off of the form

$$V_W(\mathbf{R}) = -\frac{C_0 + C_2 P_2(\cos \chi)}{(R^2 + R_c^2)^3} \quad (1)$$

where  $\mathbf{R}$  is the position of the center of Ps relative to the center of  $\text{N}_2$ ,  $\chi$  is the angle between  $\mathbf{R}$  and the internuclear axis, and  $R_c$  is a cutoff radius. The van der Waals coefficients  $C_0$  and  $C_2$  were calculated from the London formula using the polarizabilities of  $\text{N}_2$ ,  $\alpha_0=11.89$  a.u. and  $\alpha_2=4.19$  a.u. giving  $C_0 = 111.8$  a.u. and  $C_2 = 39.4$  a.u.

In order for the correlation potential to match smoothly to the asymptotic form we have chosen a cutoff radius of  $R_c = 1.08$  a.u. and for the spherical component  $\lambda = 0$  switched from the correlation potential to the asymptotic form at  $R=3.2$  a.u. In Fig. 2 we show the potential determined in this way compared with the asymptotic form at values of  $R$  between 2.5 and 4.5 a.u. for the Ps velocity of 0.01 a.u. We see that this procedure gives a smooth transition from the correlation potential to the van der Waals potential. For the non-spherical component  $\lambda = 2$  we use the same cutoff radius, but switch from the correlation potential to the van der Waals form at  $R = 5.4$  a.u. We have chosen a small velocity since this is the region in which the long range van der Waals potential has the largest effect on the scattering.

### III. IONIZATION

Apart from elastic scattering, the largest contribution to the total cross section for positronium collisions is expected to be Ps ionization (break-up). Previously we have calculated Ps ionization cross sections in collisions with molecular hydrogen [28] assuming that the  $e^- - \text{H}_2$  and  $e^+ - \text{H}_2$  scattering potentials are spherically symmetric and using the binary encounter approximation [40, 41]. This approximation, along with the pseudopotential approach to elastic Ps- $\text{H}_2$  scattering, led to total cross sections in good agreement with experimental measurements. We have also used the binary encounter approximation to calculate Ps ionization cross sections in collision with rare gas atoms Ar, Kr and Xe [29] which were in good agreement with previous calculations using the impulse approximation [42]. In this section we generalize the binary encounter approximation to non-spherical potentials.

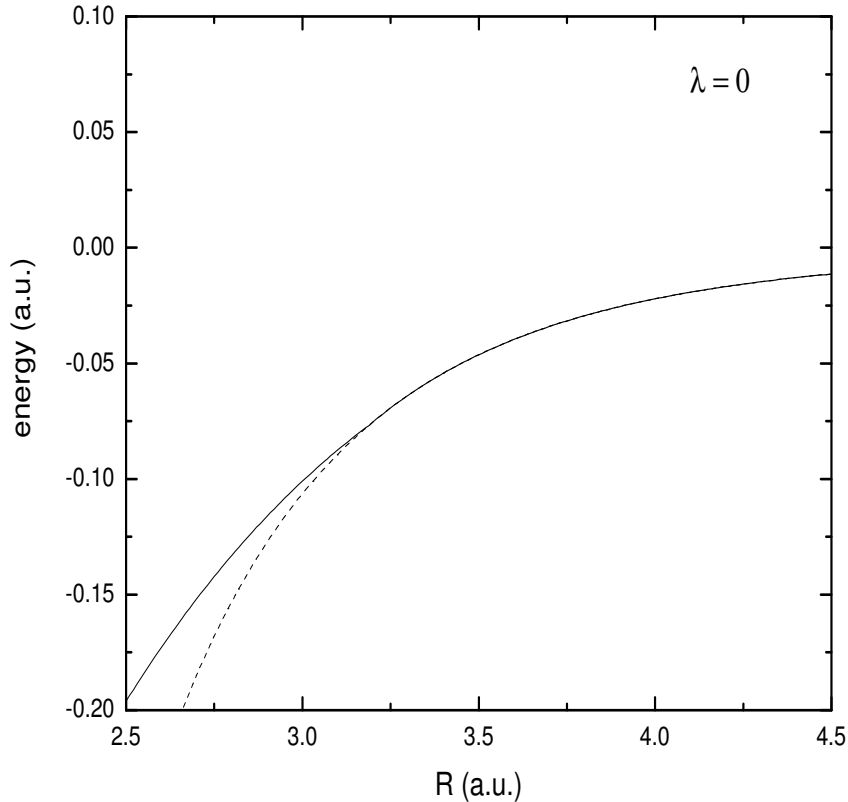


FIG. 2: Solid line: spherical component of the van der Waals potential (1). Dashed line: spherical component of the correlation potential. The van der Waals form is used for  $R > 3.2$  a.u.

### A. $e^-$ and $e^+ - \text{N}_2$ scattering

The binary encounter approximation described below depends fundamentally on the body frame  $T$ -matrix elements in the fixed-nuclei approximation for both electron and positron scattering by  $\text{N}_2$ . To calculate these scattering matrices we have used the static potential determined from the  $\text{N}_2$  ground state wave-function [39] and the Hara free electron gas exchange (HFEGE) [43] potential. We have also added a polarization potential of the form

$$V_{pol}(r) = \left[ -\frac{\alpha_0}{2r^4} - \frac{\alpha_2}{2r^4} P_2(\cos \theta) \right] C(r) \quad (2)$$

where

$$C(r) = 1 - \exp(-(r/r_c)^p). \quad (3)$$

is a cutoff function and  $r_c$  is an adjustable cutoff parameter. For both electron and positron collisions the polarization potential is attractive, but the cutoff parameter and power parameter  $p$  may be different. For electron molecule scattering it is usual to take  $p = 6$  and that is the choice we make in the present calculations. For  $e^+ - \text{N}_2$  scattering, however, calculations by Darewych [44] have shown that the choice  $p = 6$  cannot reproduce the shape of the experimentally observed cross sections below 10 eV. Later calculations by Elza *et al.* [45] using a fully adiabatic potential with  $p = 1$  provided good agreement with the experimental measurements of Hoffman *et al.* [46].

For  $e^- - \text{N}_2$  scattering we have used the wavefunction of Cade *et al.* [39] and the HFEGE exchange potential of Morrison and Collins [10]. For the polarization potential we use  $\alpha_0 = 11.78$  a.u. and  $\alpha_2 = 4.19$  a.u., and a cut-off radius of  $r_c = 2.341$  a.u which are the same values as used in [10].

In Fig. 3 (a) we show our calculated total  $e^- - \text{N}_2$  cross sections compared with the calculations of Morrison and Collins[10] and the recommended elastic cross sections of Itikawa [47]. Our results are slightly larger than that of [10] although we use the same scattering potentials. However, in our calculation, we have used partial waves up to  $l_{\text{max}} = 17$  while Morrison and Collins have used  $l_{\text{max}} = 26$ . Inclusion of more partial waves should improve the agreement between the calculations although slight numerical differences may also be responsible for some disagreement.

Both calculations are somewhat higher than the recommended elastic cross sections. This is particularly true at the position of the  $\Pi_g$  shape resonance. The reason for the large disagreement in this region is that the calculations have been done in the fixed-nuclei approximation and do not take into account the motion of the nuclei. When nuclear motion is taken into account the well known oscillatory structure [12, 13] of the cross section is seen in the region of the resonance which is not seen in a fixed-nuclei calculation.

In Fig. 3 (b) we show our calculated  $e^+ - \text{N}_2$  cross section as a function of positron velocity compared with the measurements of Hoffman *et al.* [46]. In this calculation we have used the static potential plus the adiabatic with cutoff polarization potential (ADPOS) of [45]. Our calculations are in good agreement with these calculations and the experimental values for positron velocities below 1.0 a.u.

In Fig. 4 we show  $e^- - \text{N}_2$  differential cross sections at representative scattering energies of 2.46 eV ( $v = 0.425$  a.u.) and 10 eV ( $v = 0.857$  a.u.). At 2.46 eV the cross section is at

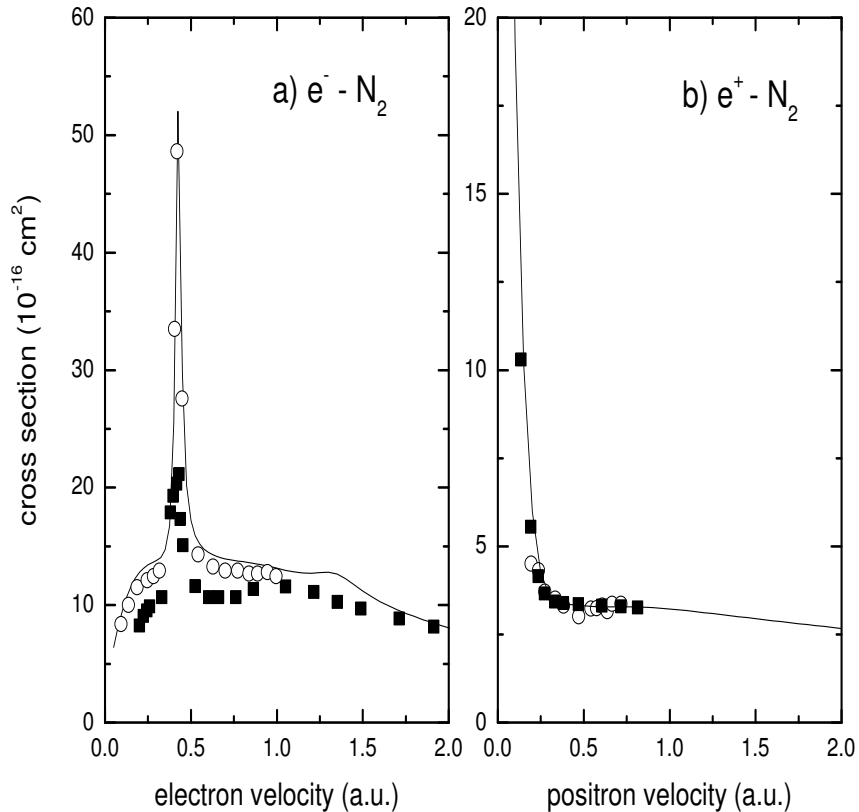


FIG. 3: (a) Total elastic  $e^- - \text{N}_2$  cross section as a function of electron velocity. Present calculation including  $\Sigma$ ,  $\Pi$  and  $\Delta$  symmetries: solid line. Calculations of Morrison and Collins [10]: open circles. Recommended elastic cross sections of Itikawa [47]: squares. b) Elastic  $e^+ - \text{N}_2$  cross sections as functions of positron velocity. Present calculation: solid line. Experimental values of Hoffman *et al.* [46]: open circles, and calculations of Elza *et al.* [45]: squares.

the peak of the  $\Pi_g$  shape resonance, and our calculated differential cross sections are much larger than the measurements and vibrational close coupling (VCC) calculations of Sun *et al.* [16]. This is again due to the fact that our calculation uses the fixed nuclei approximation in which scattering in the resonance region is dominated by the  $\Pi_g$   $T$ -matrix. When the vibrational motion is included contributions from the  $\Sigma_g$  and other symmetries become important [16] which can change the magnitude and shape of the differential cross section at and near the resonance. At 10 eV we have better agreement between experiment and the

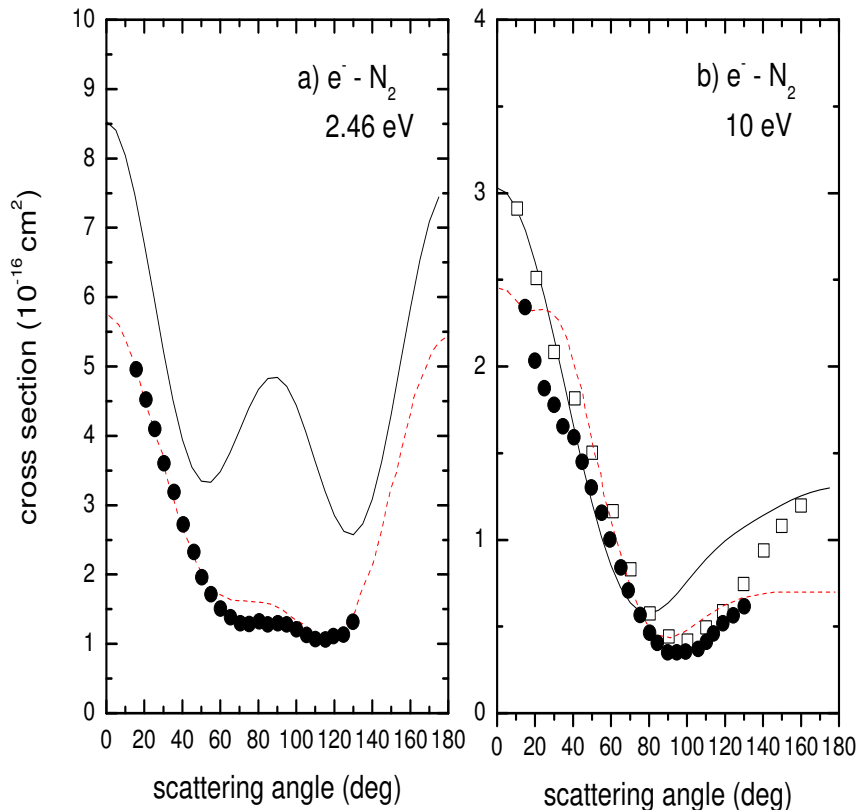


FIG. 4: (Color online)  $e^- - \text{N}_2$  differential cross sections at an incident electron energy of 2.46 eV ( $v = 0.425$  a.u.) (panel a) and 10 eV ( $v = 0.857$  a.u.) (panel b). Present fixed-nuclei calculation: solid lines. Measurements of Sun *et al.* [16]: circles. Measurements of Gote and Ehrhardt [48]: open squares. Vibrational close coupling calculations of Sun *et al.* [16]: dashed red lines.

VCC calculations, which is generally the case at energies that are not near the  $\Pi_g$  resonance.

### B. Binary encounter approximation

The binary encounter approximation is based on the assumption that the electron and positron in Ps interact independently with the target molecule and the ionization cross section due to either electron or positron collision may be written as [40]

$$\sigma_{ion}^{\pm} = \frac{1}{v_B} \langle |\mathbf{v} - \mathbf{v}_B| \int_{\Delta E > I} d\sigma^{\pm} \rangle. \quad (4)$$

where  $\mathbf{v}_B$  is the relative collision velocity,  $\mathbf{v}$  is the electron (positron) velocity relative to the Ps center-of-mass,  $d\sigma^{\pm}$  is the differential cross section for  $e^+ - B$  or  $e^- - B$  elastic scattering, and the integration is restricted by the angles which result in the energy transfer to electron (positron)  $\Delta E$  greater than the Ps ionization potential  $I = 6.8$  eV. As a result of collision with the target  $B$  the electron (positron) velocity changes from  $\mathbf{u}$  to  $\mathbf{u}'$  in the lab frame where the molecule  $B$  is at rest, so that [28]

$$\Delta E = \mathbf{v}_B \cdot (\mathbf{u} - \mathbf{u}').$$

The main difference between our present calculation of Ps ionization and our previous, spherically symmetric, calculations appears in the differential cross section. For a molecule with a ground state of  $\Sigma$  symmetry the differential cross section averaged over molecular orientation may be written in terms of the body-frame T-matrix elements as [5]

$$\frac{d\sigma}{d\Omega} = \frac{1}{4u^2} \sum_{\mu} \sum_L A_{\mu L} T_{l,l_0}^{\Lambda} T_{l',l'_0}^{\Lambda'*} P_L(\cos \theta_s), \quad (5)$$

where  $l_0, l$  are initial and final angular momenta of the scattered electron,  $\Lambda$  is its projection on the internuclear axis,  $\theta_s$  is the LAB-frame scattering angle (the angle between  $\mathbf{u}$  and  $\mathbf{u}'$ ) and  $\mu = (l, l_0, l', l'_0, \Lambda, \Lambda')$ . The coefficients result from angular momentum coupling and are given, in terms of Wigner 3-j symbols, by

$$A_{\mu L} = i^{l_0 - l + l' - l'_0} (2L + 1) [(2l_0 + 1)(2l + 1)(2l' + 1)(2l'_0 + 1)]^{1/2} \begin{pmatrix} l & l' & L \\ 0 & 0 & 0 \end{pmatrix} \\ \times \begin{pmatrix} l_0 & l'_0 & L \\ 0 & 0 & 0 \end{pmatrix} \begin{pmatrix} l & l' & L \\ \Lambda & -\Lambda' & \Lambda' - \Lambda \end{pmatrix} \begin{pmatrix} l_0 & l'_0 & L \\ \Lambda & -\Lambda' & \Lambda' - \Lambda \end{pmatrix}. \quad (6)$$

Inserting this expression for the differential cross section into (4) and performing the integration over azimuthal angles  $\phi$  and  $\phi'$  leads to an expression for the ionization cross section that is averaged over molecular orientation

$$\sigma_{ion} = \frac{\pi}{4v_B} \int_{I/2v_B}^{\infty} duu \int_{-1}^{1-I/v_B u} d(\cos \theta) |g_{1s}(u^2 + v_B^2 + 2uv_B \cos \theta)|^2$$

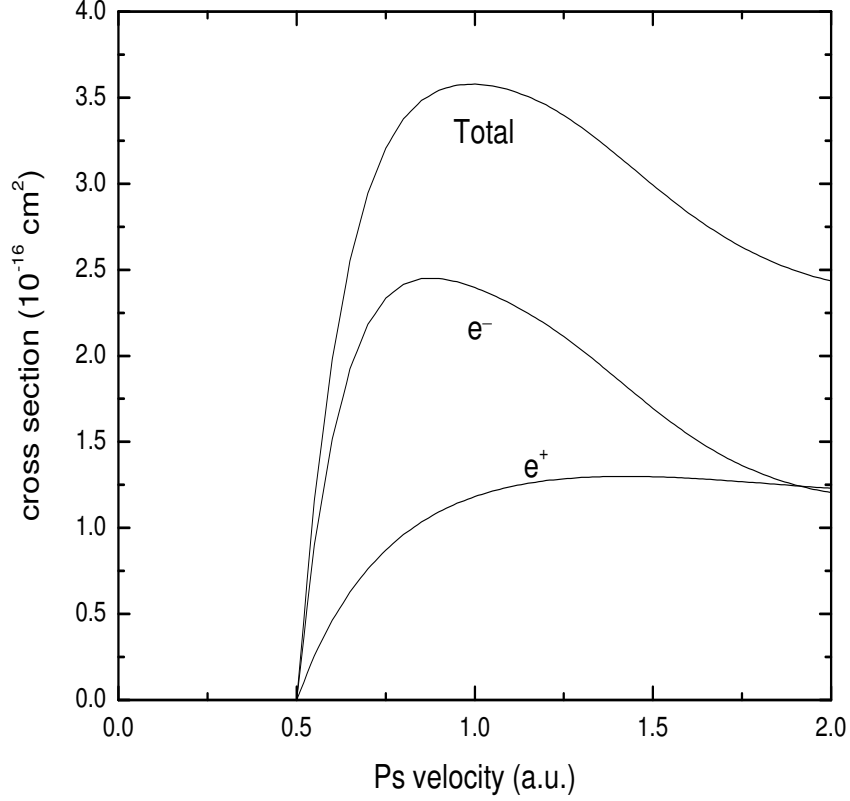


FIG. 5: Ionization of Ps by impact with  $N_2$  using the binary encounter approximation. The curve labeled 'Total' is the sum of the electron ( $e^-$ ) and the positron ( $e^+$ ) contributions.

$$\times \sum_{\mu L} A_{\mu L} T_{l,l_0}^{\Lambda} T_{l',l'_0}^{\Lambda'*} P_L(\cos \theta) \int_{\cos \theta + I/v_B u}^{\cos \theta + v_B/u} d(\cos \theta') P_L(\cos \theta') \quad (7)$$

where  $|g_{1s}|^2$  is the velocity distribution of the electron (positron) in Ps given by

$$\frac{1}{4\pi} |g_{1s}(v^2)|^2 = \frac{1}{4\pi} \frac{256}{\pi(4v^2 + 1)^4}.$$

The integration limits follow from the restriction that  $\Delta E > I$  [28, 29].

In Fig. 5 we present the total ionization cross section and contributions due to electron and positron. At velocities near threshold the electron contribution is dominant, but at higher velocities the electron contribution decreases and the positron contribution remains flat until they become comparable around 1.8 a.u. This happens because as the Ps velocity

increases,  $v_B$  in equation (7), the lower limit on the integration over  $u$ , the positron velocity, gets closer to zero, but in this region the positron cross section is rapidly increasing. The situation is different from what we see in the case of rare-gas atoms [29] and  $H_2$  [28] where the electron contribution remains dominant for all Ps velocities.

#### IV. RESULTS AND DISCUSSION

In order to obtain fixed nuclei  $T$ -matrices for Ps scattering we solve the set of coupled equations describing Ps- $N_2$  scattering using the integral equation method [49]. From these  $T$ -matrices we obtain the elastic cross section that is averaged over molecular orientation.

In Fig. 6 we present our theoretical elastic, ionization and total cross sections, and compare the latter with the experimental data [1, 4]. The theoretical resonance peak's position ( $v = 0.34$  a.u.) is slightly shifted towards lower Ps velocities relative to the experimental peak position ( $v = 0.46$  a.u.) The latter might be due to the the fixed nuclei-approximation which does not take into account the vibrational dynamics. However, there is a secondary peak at a slightly higher velocity of  $v = 0.44$  a.u. In our previous calculations [30], a significant difference between the theory and experiment was observed at higher velocities where the experimental cross section remains practically flat and stays close to the  $e-N_2$  cross section, whereas the theoretical curve was showing a relatively fast decrease with growing  $v$ . A similar tendency was observed in Ps- $H_2$  calculations [28]. The present calculations which take into account short-range correlations agree much better with the measurements at higher velocities.

In order to understand the composition of the resonance peaks we show, in Fig. 7, the partial cross sections for the scattering symmetries included in our calculation of the total elastic cross section. Unlike the case of  $e^-N_2$  scattering we do not see the resonance in the  $\Pi_g$  symmetry, but see a peak in the  $\Delta_g$  partial cross section which is responsible for the maximum in the total cross section at  $v = 0.34$  a.u. and a peak in the  $\Pi_u$  partial cross section which is mainly responsible for the maximum in the total cross section at  $v = 0.44$  a.u. We should note though that the actual dependence of the cross section on Ps energy should be more complicated, since inclusion of vibrational motion of the target will create additional structure in the cross section (boomerang oscillations [13]) which is not resolved yet in measurements [1, 4].

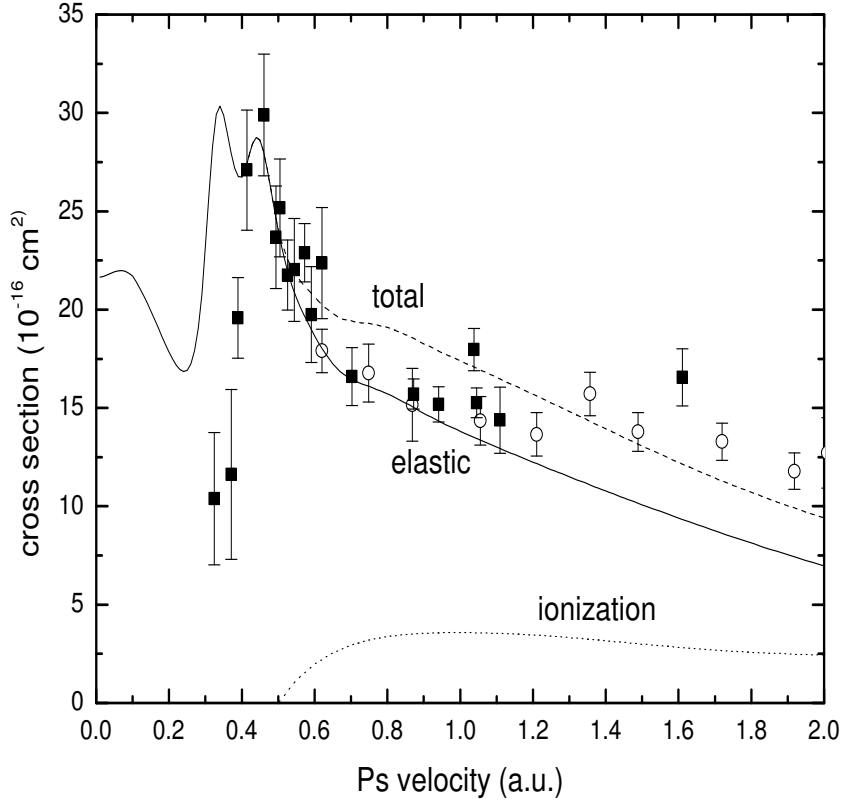


FIG. 6: Cross sections for Ps scattering with  $N_2$ . Theory: Solid line, elastic cross section; dashed line, total cross section; dotted line, ionization cross section. Experiment: squares, Brawley *et al.* [1]; open circles, Shipman *et al.* [4].

These differences from  $e^-$ - $N_2$  scattering can be understood by looking at the spherically symmetric ( $\lambda=0$ ) components of the potential and considering some of dominant potential matrix elements  $V_{LL}^M$ . For the spherically symmetric component there is no  $d$ -wave resonance, in fact the potential supports a weakly bound state. Also there is an  $f$ -wave shape resonance. When anisotropy is included in the potential ( $\lambda$  is increased) the  $\Sigma_g$  matrix element  $V_{22}^0$  becomes more attractive. In the  $\Delta_g$  symmetry the matrix element  $V_{22}^2$  becomes weaker and the bound state moves into the continuum and a resonance appears in this symmetry. For the  $\Pi_g$  symmetry the matrix element  $V_{22}^1$  does not change very much as anisotropy is included and we do not see a resonance appear. The peak at  $v = 0.44$  a.u. is

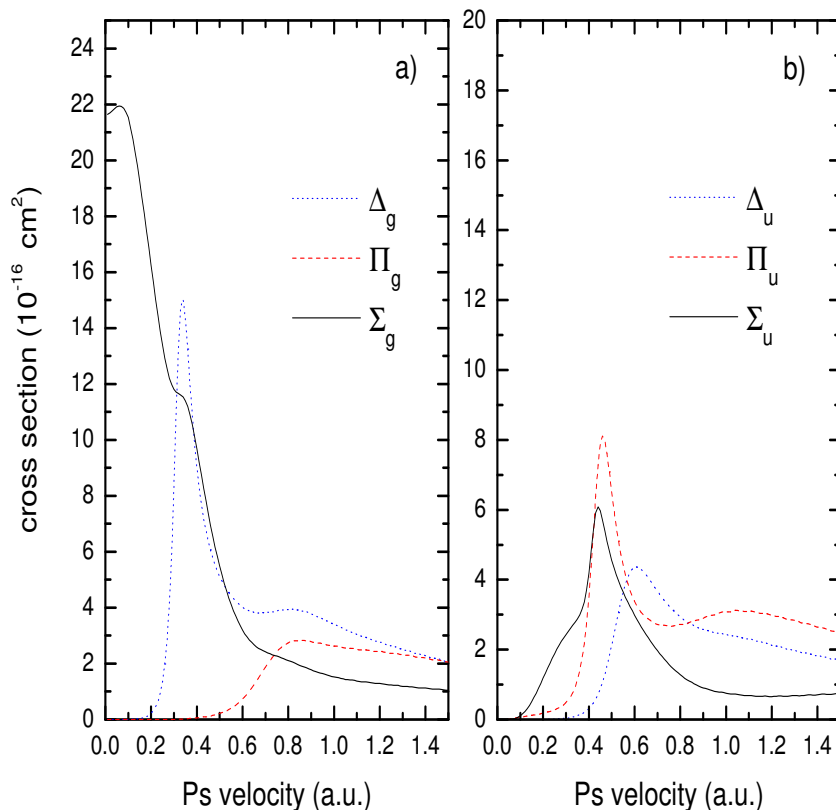


FIG. 7: (Color online) Partial cross sections for Ps-N<sub>2</sub> elastic scattering a) even (gerade) scattering symmetries. b) odd (ungerade) scattering symmetries.

related to the  $f$ -wave resonance that is seen in the scattering by the spherically symmetric component of the potential.

Again this is quite different from  $e^-$ -N<sub>2</sub> scattering where a  $d$ -wave resonance is seen even for the spherically symmetric component of the scattering potential and becomes stabilized in the  $\Pi_g$  symmetry as anisotropy is included. However, it might be expected that the composition of resonances for Ps scattering might be more sensitive to the inclusion of anisotropy than in electron scattering due to the vanishing of the static potential for Ps scattering. Finally, but perhaps most importantly, since the Ps electron is bound, there is no one-to-one correspondence between the electron angular momentum in electron scattering and Ps angular momentum in Ps scattering.

Analysis of the low-energy behavior of the  $\Sigma_g$  phase shifts shows that the scattering length for Ps-N<sub>2</sub> scattering is  $A = 2.49$  a.u. This indicates the absence of the Ramsauer-Townsend minimum, similar to the case of Ps scattering by rare gas atoms [27, 29]. The dip at  $v = 0.25$  a.u. is due to the resonance behavior of the  $\Delta_g$  contribution which peaks at  $v = 0.34$  a.u. while the  $\Sigma_g$  contribution is decreasing.

Overall, the  $\Sigma_g$  contribution seems to be too large at low energies. This might be caused by an error in the short-range part of the exchange and correlation potentials [38]: due to the strong dependence of the electron density on electron coordinate near the target nuclei, replacing the Fermi momentum by  $[3\pi^2n(\mathbf{R})]^{1/3}$  could be inaccurate.

## V. CONCLUSION

In conclusion we have constructed new FEG exchange and correlation potentials allowing us to describe resonant Ps-N<sub>2</sub> scattering similar to the  $e$ -N<sub>2</sub> resonant scattering in the  $\Pi_g$  symmetry. These potentials were determined from the FEG exchange and correlation energies calculated in the preceding paper [38] by using the Thomas-Fermi model to introduce the dependence of the energy on the distance between the projectile and the target. Although the composition of the Ps-N<sub>2</sub> resonance is more complex, our results further confirm the observed similarity between electron and Ps scattering which can be extended now towards resonance phenomena. The position of the resonance peak is slightly below the observed position. This could be due to the neglect of nuclear motion. Therefore the next step in theoretical development should be incorporation of vibrational dynamics along the lines of the boomerang model [13]. This also opens an opportunity of calculations of vibrational excitation cross sections in Ps-N<sub>2</sub> collisions.

In previous calculations for rare-gas atoms [27, 29] we constructed a pseudopotential with a repulsive core to mock the orthogonality condition. In the present calculation we do not add a repulsive core to the FEG potentials. Recent measurements of Ps-rare gas scattering at low velocities [50] show a decrease in the cross section in this region. The pseudopotential calculations as well as other recent calculations [36, 37] do not exhibit such a decrease. Therefore it is natural that as a next step we plan to apply the present method to Ps scattering by heavy-rare gas atoms. Future application of the present method to Ps scattering by other molecules, such as CO<sub>2</sub> where a resonance in Ps scattering has also been

observed [2], is of interest as well.

### Acknowledgments

The authors are grateful to Gleb Gribakin for many useful comments. This work was partly supported by the US National Science Foundation under Grant No. PHY-1401788.

- 
- [1] S. J. Brawley, S. Armitage, J. Beale, D. E. Leslie, A. I. Williams, and G. Laricchia, *Science* **330**, 789 (2010).
  - [2] S. J. Brawley, A. I. Williams, M. Shipman, and G. Laricchia *Phys. Rev. Lett.* **105**, 263401 (2010).
  - [3] S. J. Brawley, A. I. Williams, M. Shipman, and G. Laricchia, *J. Phys.: Conf. Series* **388**, 012018 (2012).
  - [4] M. Shipman, S. J. Brawley, L. Sarkadi, and G. Laricchia, *Phys. Rev. A* **95**, 032704 (2017).
  - [5] N. F. Lane, *Rev. Mod. Phys.* **52**, 29 (1980).
  - [6] P. G. Burke and A.-L. Sinfailam, *J. Phys. B* **3**, 641 (1970).
  - [7] P. G. Burke and N. Chandra, *J. Phys. B* **5**, 1696 (1972).
  - [8] M. A. Morrison and B. I. Schneider, *Phys. Rev. A* **16**, 1003 (1977).
  - [9] B. D. Buckley and P. G. Burke, *J. Phys. B* **10**, 725 (1977).
  - [10] M. A. Morrison and L. A. Collins, *Phys. Rev. A* **17**, 918 (1978).
  - [11] B. I. Schneider, *Phys. Rev. A* **24**, 1 (1981).
  - [12] A. Herzenberg, *J. Phys. B* **1**, 548 (1968).
  - [13] D. T. Birtwistle and A. Herzenberg, *J. Phys. B* **4**, 53 (1971).
  - [14] N. Chandra and A. Temkin, *Phys. Rev. A* **13**, 188 (1976).
  - [15] B. I. Schneider, M. Le Dourneuf, and Vo Ky Lan, *Phys. Rev. Lett.* **43**, 1926 (1979).
  - [16] W. Sun, M. A. Morrison, W. A. Isaacs, W. K. Trail, D. T. Alle, R. J. Gulley, M. J. Brennan, and S. J. Buckman, *Phys. Rev. A* **52**, 1229 (1995).
  - [17] H. Feng, W. Sun, and M. A. Morrison, *Phys. Rev. A* **68**, 062709 (2003).
  - [18] H. Hotop, M.-W. Ruf, M. Allan, and I. I. Fabrikant, *Adv. At. Mol. Phys.* **49**, 85 (2003).
  - [19] I. I. Fabrikant, S. Eden, N. J. Mason and J. Fedor, *Adv. At. Mol. Opt. Phys.* **66**, 546 (2017).

- [20] L. Sarkadi, Phys. Rev. A **68**, 032706 (2003).
- [21] J. Mitroy and I. A. Ivanov, Phys. Rev. A **65**, 012509 (2001).
- [22] J. Mitroy and M. W. J. Bromley, Phys. Rev. A **67**, 034502 (2003).
- [23] I.A. Ivanov, M. W. J. Bromley, and J. Mitroy, Comp. Phys. Comm. **152**, 9 (2003).
- [24] P. K. Biswas and S. K. Adhikari, Phys. Rev. A **59**, 363 (1999).
- [25] S. K. Adhikari and P. K. Biswas, Phys. Rev. A **59**, 2058 (1999).
- [26] P. K. Biswas and S. K. Adhikari, Chem. Phys. Lett. **317**, 129 (2000).
- [27] I. I. Fabrikant and G. F. Gribakin, Phys. Rev. A **90**, 052717 (2014); *ibid.* **97**, 019903(E) (2018).
- [28] R. S. Wilde and I. I. Fabrikant, Phys. Rev. A **92**, 032708 (2015).
- [29] G. F. Gribakin, A. R. Swann, R. S. Wilde, and I. I. Fabrikant, J. Phys. B **49**, 064004 (2016).
- [30] I. I. Fabrikant, G. F. Gribakin and R. S. Wilde, J. Phys. Conf. Series **875**, 012001 (2017).
- [31] G. Laricchia and H. R. J. Walters, Riv. Nuovo Cimento **35**, 305 (2012).
- [32] C. P. Campbell, M. T. McAlinden, F. G. R. S. MacDonald, and H. R. J. Walters, Phys. Rev. Lett. **80**, 5097 (1998).
- [33] J. E. Blackwood, M. T. McAlinden, and H. R. J. Walters, Phys. Rev. A **65**, 032517 (2002).
- [34] J. E. Blackwood, C. P. Campbell, M. T. McAlinden, and H. R. J. Walters, Phys. Rev. A **60**, 4454 (1999).
- [35] J. E. Blackwood, M. T. McAlinden, and H. R. J. Walters, J. Phys. B **35**, 2661 (2002).
- [36] A. R. Swann and G. F. Gribakin, Phys. Rev. A **97**, 012706 (2018).
- [37] D. G. Green, A. R. Swann, and G. F. Gribakin, <https://arxiv.org/pdf/1709.00394>
- [38] I. I. Fabrikant and R. S. Wilde, Phys. Rev. A, preceding paper
- [39] P. E. Cade, K. D. Sales, and A. C. Wahl, J. Chem. Phys. **44**, 1973 (1966).
- [40] B. M. Smirnov, in *The Physics of Electronic and Atomic Collisions*, eds. J. S. Risley and R. Geballe (University of Washington Press, Seattle, 1976), p. 701.
- [41] M. R. Flannery, in *Rydberg States of Atoms and Molecules*, eds. R. F. Stebbings and F. B. Dunning (Cambridge University Press, Cambridge 1983), p. 393.
- [42] C. Starrett, M. T. McAlinden, and H. R. J. Walters, Phys. Rev. A **72**, 012508 (2005).
- [43] S. Hara, J. Phys. Soc. Japan **22**, 710 (1967).
- [44] J. W. Darewych, J. Phys. B **15** L415 (1982).
- [45] B. K. Elza, T. L. Gibson, M. A. Morrison, B. C. Saha, J. Phys. B **22**, 113 (1989).

- [46] K. R. Hoffman, M. S. Dabaneh, Y. F. Hsieh, W. E. Kaupilla, V. Pol, J. H. Smart and T. S. Stein, *Phys. Rev. A* **25** 1393 (1982).
- [47] Y. Itikawa, *J. Phys. Chem. Ref. Data* **35** 31 (2006).
- [48] M. Gote and H. Ehrhardt, *J. Phys. B* **28** 3957 (1995).
- [49] M. A. Morrison, in *Electron-Molecule and Photon-Molecule Collisions*, eds. T. Rescigno, V. McKoy and B. Schneider (Plenum Press, New York 1979), p. 15.
- [50] S. J. Brawley, S. E. Fayer, M. Shipman and G. Larricchia, *Phys. Rev. Lett.* **115** 223201 (2015).